D4.2 Application of holography to dense steerable antennas, optimization of recognition beams

Grant Agreement Number	101099491
Action Acronym	HOLDEN
Action Title	Ethical Design of Holography with Dense wireless Networks (HOLDEN)
Funding Scheme	HORIZON-EIC-2022-PATHFINDEROPEN-01
Version date of the Annex I against which the assessment will be made	13/12/2022
Start date of the project	1/6/2023
Due date of the deliverable	28/02/2025
Actual date of submission	28/02/2025
Responsible	CNR
Contributors	CNR, POLIMI, TUM
Dissemination level	Public (dataset description)

European Innovation Council

Funded by the European Union

Funded by the European Union. Views and opinions expressed are, however, those of the author(s) only and do not necessarily reflect those of the European Union or European Innovation Council and SMEs Executive Agency (EISMEA). Neither the European Union nor the granting authority can be held responsible for them. Grant Agreement No: 101099491.

Authors in alphabetical order

Full Name	Organisation	E-mail
Michele d'Amico	POLIMI	michele.damico@polimi.it
Thomas Eibert	TUM	eibert@tum.de
Federica Fieramosca	POLIMI	federica.fieramosca@polimi.it
Sanaz Kianoush	CNR	sanaz.kianosuh@cnr.it
Usevalad Milasheuski	CNR	usevaladmilasheuski@cnr.it
Han Na	TUM	han.na@tum.de
Alexander Paulus	TUM	a.paulus@tum.de
Vittorio Rampa	CNR	vittorio.rampa@ieiit.cnr.it
Matthias Saurer	TUM	matthias.saurer@tum.de
Stefano Savazzi	CNR	stefano.savazzi@cnr.it
Quanfeng Wang	TUM	quanfeng.wang@tum.de

Change History

Version	Date	Status	Author (Company)	Description
1.0	9/01/2025	Revision	CNR	First draft
2.0	18/1/2025	Revision	TUM	Second draft
3.0	23/1/2025	Revision	POLIMI	Second draft revised
4.0	30/1/2025	Final	CNR	Final draft comments
5.0	13/02/2024	Final revision	ALL	Final version

Executive Summary

The deliverable presents experimental and simulated datasets both collected with the purpose of:

1) applying holography to dense steerable antennas

2) assessing human body blockage in both dense 2D and 3D arrays

3) presenting an initial application of holography tools in practical WiFi devices (with limited number of antenna, carriers and beams).

The following contents are covered in this report:

- Short introduction of the HOLDEN project and the collaboration partners
- Measurement dataset and description of the indoor measurement campaign. The proposed measurement dataset is obtained from a planar scanner and are used for the assessment of human body blockage in dense 2D arrays
- Initial WiFi CSI data collected in a representative indoor environment which is used for testing recognition algorithms implementations as well to select optimized beams

The datasets considered in this deliverable have been also used to validate the signal processing and hologram frame management tools, namely the generative AI methods, as detailed in D3.6.

Finally, the deliverable also reports an initial implementation of Multiple Signal Classification – (MUSIC) tool which is adopted to disentangle the multipath components of the CSI and optimize the recognition beams. Further implementation and refinement of the algorithms will be the focus of the deliverable D6.4, informed by the results of the ADANT test house measurement campaign.

Table of Contents

Abbreviations **5**

1. Introduction **6**

1.1. About HOLDEN 6

1.2. Partners 6

2. Human body blockage measurements from a planar scanner: data structure **8**

3. Measurements – Planar Office Scanner **9**

3.1. Public Link 9

3.2. Description and Visualization 9

4. WiFi CSI frame datasets for body motion discrimination **14**

4.1. Public link 14

4.2. WiFi devices and Channel Quality Information 16

4.3. Folders and CSV files 17

4.4. File and columns CSI datasets descriptions 17

5. References **19**

6. Table of Figures **20**

Abbreviations

Abbreviation	Description
3D	Three-dimensional
Aalto	Aalto University
BPA	back-projection algorithm
CNR	Consiglio Nazionale Ricerche
DOA	Direction of Arrival
EC	European Commission
EM	electromagnetic
ESM	Ethics Status Monitor
EU	European Union
HOLDEN	ethical design of holography in dense wireless networks
MUSIC	Multiple Signal Classification
MoM	method of moments
PEC	perfectly electrically conducting
POLIMI	Politecnico di Milano
RF	radio frequency
TOI	target of interest
TUM	Technical University of Munich
TWE	University of Twente
UAV	uninhabited aerial vehicle
VNA	vector network analyzer
WP	work package

1. Introduction

1.1. About HOLDEN

The ubiquitous perception by sensing of objects, subjects and gestures is a pivotal challenge for future technology: it enables personalized services such as smart living, automated logistics or interaction through free-space gestures. However, it also challenges ethical and moral boundaries and threatens privacy. HOLDEN proposes a radically new approach to perception by concisely analysing ethical constraints and privacy risks while re-thinking RF-based sensing. We establish necessary conditions for privacy preserving and ethically compliant sensing and develop new paradigms respecting these constraints.

For the first time ever, HOLDEN constitutes a concentrated effort to explore social aspects of RF-sensing to guide the technological advance and to derive technology for ethically and privacy compliant perception. Central to HOLDEN is the development of ethical and privacy constraints. We use these findings to derive privacy and ethically compliant concepts for RF-based perception. We will develop a system of distributed multi-antenna devices for simultaneous multitarget recognition and ubiquitous perception with unprecedented accuracy, which constitutes a radical paradigm shift from a technology-centric perspective to a privacy-centric one via privacy by design.

HOLDEN achieves this goal along three high risk, complementary, and privacy-centric paths:

Path 1: Continuous-space measurement points: Radio-based 3D vision by holographic image processing of RF wavefronts.

Path 2: Discrete-space measurement points: Advanced 3D beamforming for human-scale recognition and tracking through dense massive, connected antenna arrays.

Path 3: Signal processing and learning: High-dimensional tensor processing for the distinction of complex activities and motion from massive-dimensional RF data. The resulting breakthrough approaches and algorithms will be compared against application-level benchmarks via usage scenarios in the fields of logistics, smart living, and free-space

1.2. Partners

The consortium consists of four academic partners and a high-tech SME partner: (a) Aalto University (AALTO), Finland, (b) Technical University of Munich (TUM), Germany, (c) Consiglio Nazionale Ricerche (CNR), with third party Politecnico di Milano (POLIMI), Italy, (d) University of Twente (TWE), Netherlands, and (e) Adant (Adant), Italy. This consortium features the specialized and complementary expertise required to achieve the project objectives. AALTO will be responsible for the project management (WP1), covered by an experienced and dedicated project manager. Ethical aspects (WP2) will be addressed by TWE (Prof. Ciano Aydin) who is a pioneer in the field. Eventual gender differences in the ethical perception will be taken into account. TUM pioneered RF holography, which makes TUM (Prof. Thomas Eibert) the ideal leader of WP3. In advanced distributed signal and information processing, CNR has through Prof. Stefano Savazzi more than

14 years of experience. CNR will lead WP4. Since more than 10 years, AALTO is active in radio sensing and machine learning based activity recognition. This expertise makes AALTO (Prof. Sigg) the ideal leader of WP5. Adant (Daniele Piazza) will contribute to the market analysis, application possibilities, and validation (WP6). Led by AALTO, dissemination with the website as one the media will be addressed by all partners. All academic partners are committed to early publication of results, e.g., via arXiv (open science).

2. Human body blockage measurements from a planar scanner: data structure

The open-source database contains the following type of files.

- ***mannequin_[Filename*]*.mat:** Continuous wave measurement data from a planar scanner. The data is stored in MATLAB **Error! Reference source not found.** data format. The transmission and reflection coefficients between a fixed transmit antenna and a moving (on the planar scanner) antenna, both vertically polarized, are measured for three arrangements of mannequins within a typical office environment.
    - **freqs [21x1]**: frequencies of measurements
    - **S11 [162x80x21]**: complex-valued reflection coefficient for each measurement location and frequency
    - **S21 [162x80x21]**: complex-valued transmission value for each measurement location and frequency
    - **X/Y [162x80]**: x- and y-location of the measurement samples

3. Measurements – Planar Office Scanner

3.1. Public Link

A public link to the dataset is provided as follows:

Q. Wang, A. Paulus, H. Na, M. M. Saurer, and T. F. Eibert, "RF holography and perception in static environments: Dataset," Oct. 2024. Zenodo. https://doi.org/10.5281/zenodo.13981780

3.2. Description and Visualization

A two-axis planar scanning system has been installed on a side wall of a typical office room at the Chair of High-Frequency Engineering, Department of Electrical Engineering, School of Computation, Information and Technology of the Technical University of Munich. The setup, of which a photograph is shown in Fig. 1, allows the acquisition of the radio transmission (S_{21} parameter acquired with a VNA) between a fixed transmit antenna (vertically/y-polarized) and a moving probe antenna (vertically/y-polarized), which is moved by the scanner system on a surface of approximately 4.98 m x 2.46 m (excluding margins for safety). The transmission between both antennas is recorded within the frequency range from 2.4 GHz to 2.5 GHz, where the surface of the wall is sampled with a resolution of approximately 3 cm, resulting in 162 x 80 = 12960 samples for a full measurement. All measurements have been performed in a step-mode manner, where a S_{21} sample is recorded after moving the probe to a desired x- and y-position and waiting for vibrations of the platform to decay. A full measurement takes around 17 hours and overall 68 full measurements have been acquired, leading to an equivalent measurement time of approximately 51 days of continuous operation. A NanoVNA600A [1] was used for all measurements, where additional amplifiers and filters have been added in the signal path. The raw data of a typical measurement is shown in Fig. 2, where the wave-like behavior in the phase data already indicates the presence of a dominant radiation source.

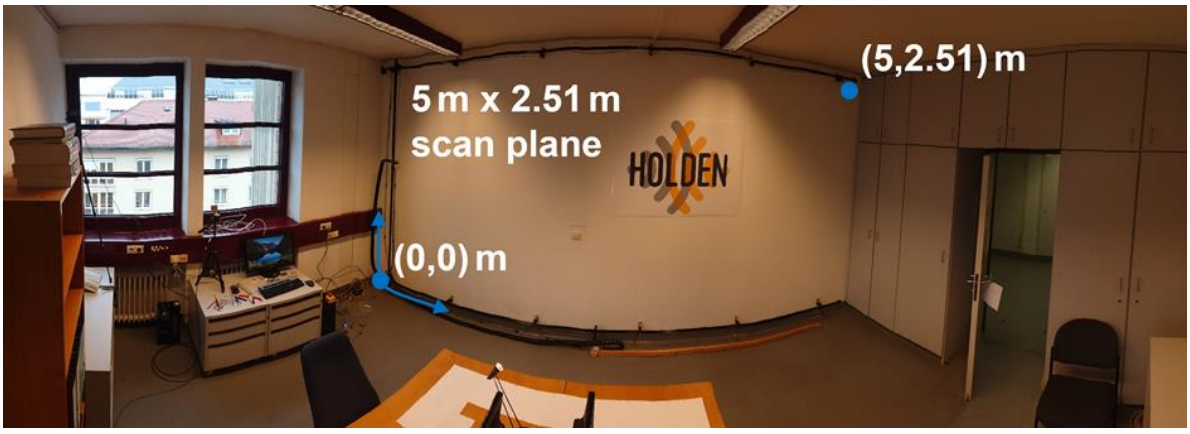

Fig. 1. Wide-angle photograph of the planar scanner (dense 2D array of antennas) installed in an office at TUM.

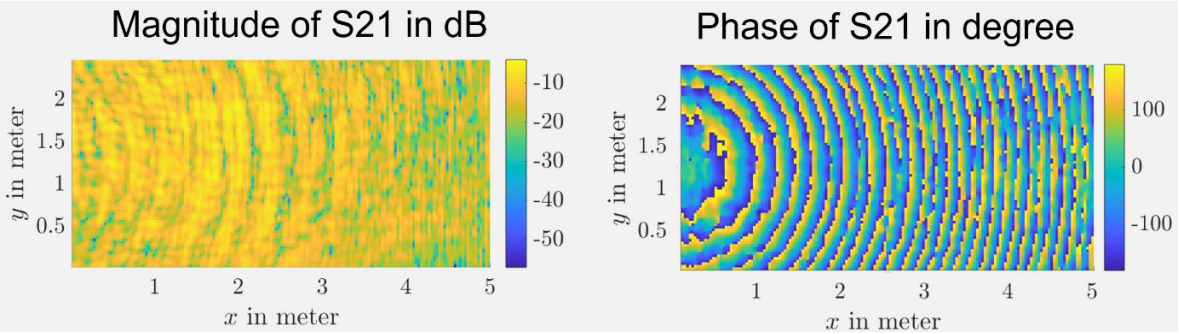

Fig. 2. Typical measured transmission data within the office environment. Illustration of the magnitude of the transmission (left) in dB and the corresponding phase information (right) in degree.

The 68 different measurements belong to different arrangements of plastic/wooden mannequins (shown in Fig. 3) within the office. In order to reassemble the interaction between electromagnetic waves in the low-GHz frequency range with real human bodies as closely as possible, the mannequins where painted with zinc-aluminium spray before being employed in the measurement campaign (not shown here). This zinc-aluminium paint was found to be a suitable and cheap alternative to silver- or copper-based conductive paints.

Further details, images and explanations of the measurement setup and hardware are provided in the "TUM_HFT_WiFi_Mannequins_Documentation_Public_12_09_2024.pptx" file, which is available in the public repository.

Fig. 3. Female and male mannequins used for the measurements.

The measurement data is provided in the form of MATLAB [2] files, which contain the following variables:

- **freqs [21x1]**: frequencies of measurements
- **S11 [162x80x21]**: complex-valued reflection coefficient for each measurement location and frequency (made available mostly for the reason of completeness, usability limited)
- **S21 [162x80x21]**: complex-valued transmission value for each measurement location and frequency
- **X/Y [162x80]**: x- and y-location of the measurement samples

Each measurement file belongs to a measurement arrangement which is shown in the accompanying "TUM_HFT_WiFi_Mannequins_Documentation_Public_12_09_2024.pptx" file, where either none, one or two mannequins are present within the room, and are fixed to exhibit different gestures or poses.

To further illustrate the measurement setup and gestures performed by the mannequins, two videos consisting of sequences of snapshots acquired from a webcam and surveilling the measurement arrangement are provided in the files "Exemplary_measurement.mp4" and "Start_positions.mp4". The latter file shows the interior of the room, i.e., the arrangement of the mannequins (if present) and furniture, of each measurement dataset. The "Exemplary_measurement.mp4" showcases the process of a single measurement, in the form of a time lapse, and consists of snapshots taken at every 100th measurement location.

An example of the scattering information obtainable when processing the difference between two successive measurements is shown in Fig. 4. On the top half of the figure, a three-dimensional point cloud, also shown in terms of three projections to cut-planes through the room, is illustrated. Only the dominant scattering centers are drawn, which is obtained by a simple thresholding scheme of the difference image. By processing the difference between two measurements, the (assumed to be) constant illumination and contributions from objects, which are unchanged between the measurements, are almost completely removed. This allows for a clearer illustration and investigation of the regions of interest, namely objects which are moving "over time", i.e., which change their position, shape or orientation between the measurements. However, due to instabilities in the measurement equipment, mostly the VNA, and the limited repeatability of the mechanical setup, a perfect cancellation of constant contributions is not achieved, leading to additional "noise" in the reconstructed scenario. Nevertheless, in the top of Fig. 4, the male mannequin, and, in particular, its left arm, can be rather sharply localized in the xy-projection. The rest of the room, including the female mannequin, has not been modified in between the two measurements and, thus, should not be visible in the image. Since the xy-plane coincides with the plane of the measurement surface, the accuracy of the image in this projection is expected to be the highest among the depicted planes. Furthermore, ignoring strong scattering centers at values of z close to 0.2 m, the approximate distance of the left arm of the male mannequin with respect to the planar scanner can be read as approximately 1.7 m from the xz-projection. Lastly, the least accurate information can be obtained from the yz-projection. A photograph of the arrangement of the mannequins within the room is show in the bottom half of Fig. 4. In general, it is

recommended to investigate sequences of measurements, as the result images, combined in the form of a video, allow for a more intuitive interpretation by human observers.

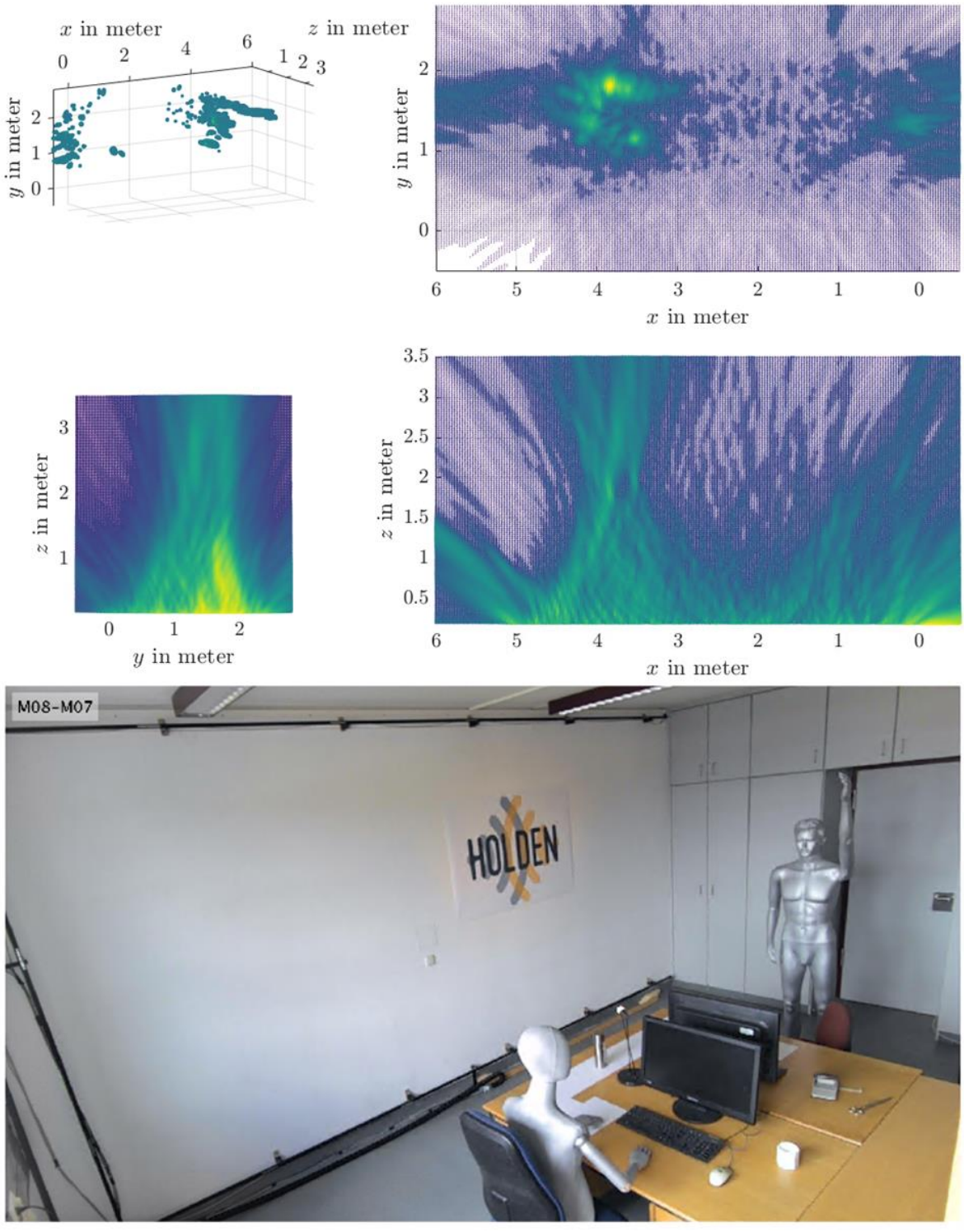

Fig. 4. Illustration of a holographic three-dimensional image generated from the difference of the datasets “mannequin_08_04_06_2024.mat” and “mannequin_07_03_06_2024.mat”. On the top, a point-cloud illustration of the dominant scatterers is shown. Projections to the plane of

the measurement surface (xy-plane, top-right-top), a vertical cut (xz-plane, top-right-bottom) and a cross-section projection (yz-plane, top-left-bottom) are provided. The arrangement of measurement “mannequin_08_04_06_2024” is shown in the photograph on the bottom.

4. WiFi CSI frame datasets for body motion discrimination

This second dataset serves to investigate the impact of human body blockage on practical WiFi chipsets which support channel state/quality information (CSI) measurements obtained by a multiple input multiple output system. The goal is to track human body blockage effects on WiFi baseband channel impulse response. The dataset serves as an initial setup which is useful to test scenario that will be assessed in ADANT testhouse (WP6).

The experimental activities have been conducted inside an indoor lab environment having size 6 × 4 sqm.

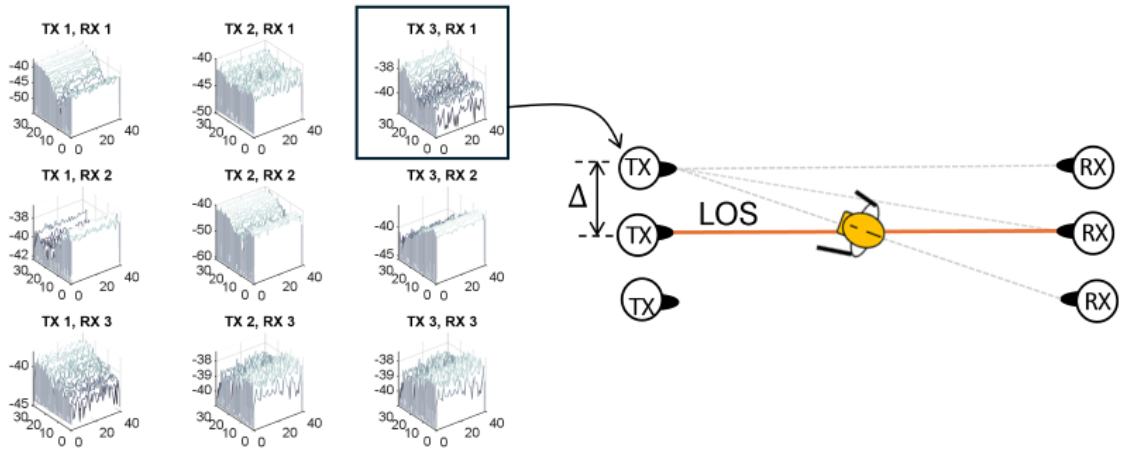

Fig. 5. Illustration of the CSI data structuring of a MIMO WiFi link. 3D CSI structures are defined in terms of frequency (subcarriers), symbols and antennas (TX-RX pair).

As shown in the Figure 5 above, a single MIMO WiFi device is acting as TX and being equipped with 3 antennas, the RX is also equipped with 3 antennas. Distance between the TX and RX is 210 cm. The TX is located 61 cm above ground. The RX is located 74 cm above ground. Devices are deployed in the monitored area to capture the target (human body) presence and its activity inside the room environment.

4.1. Public link

Public link to dataset is available

Stefano Savazzi, Sanaz Kianoush, and Vittorio Rampa. (2024). WiFi frame datasets for body motion discrimination [Data set]. Kaggle. DOI: 10.34740/kaggle/ds/4802891

https://www.kaggle.com/datasets/rvision/wifi-frame-datasets-for-body-motion-discrimination

Multiple Signal Classification (MUSIC) algorithm is used to disentangle the multipath components of the CSI and monitor any changes of such components possibly induced by body movements. MUSIC algorithm is thus used to recognize beams that may be influenced by body motions.

The **source code and software** to test the MUSIC processing system (see [2] for a general definition) is published online as part of the dataset and is available in the following:

https://www.kaggle.com/code/rvision/simple-music-spectrum-evaluation-example

The code can be edited and run in real time (see also the screenshot examples in Figure 6):

https://www.kaggle.com/code/scratchpad/notebooke65827e67c/edit

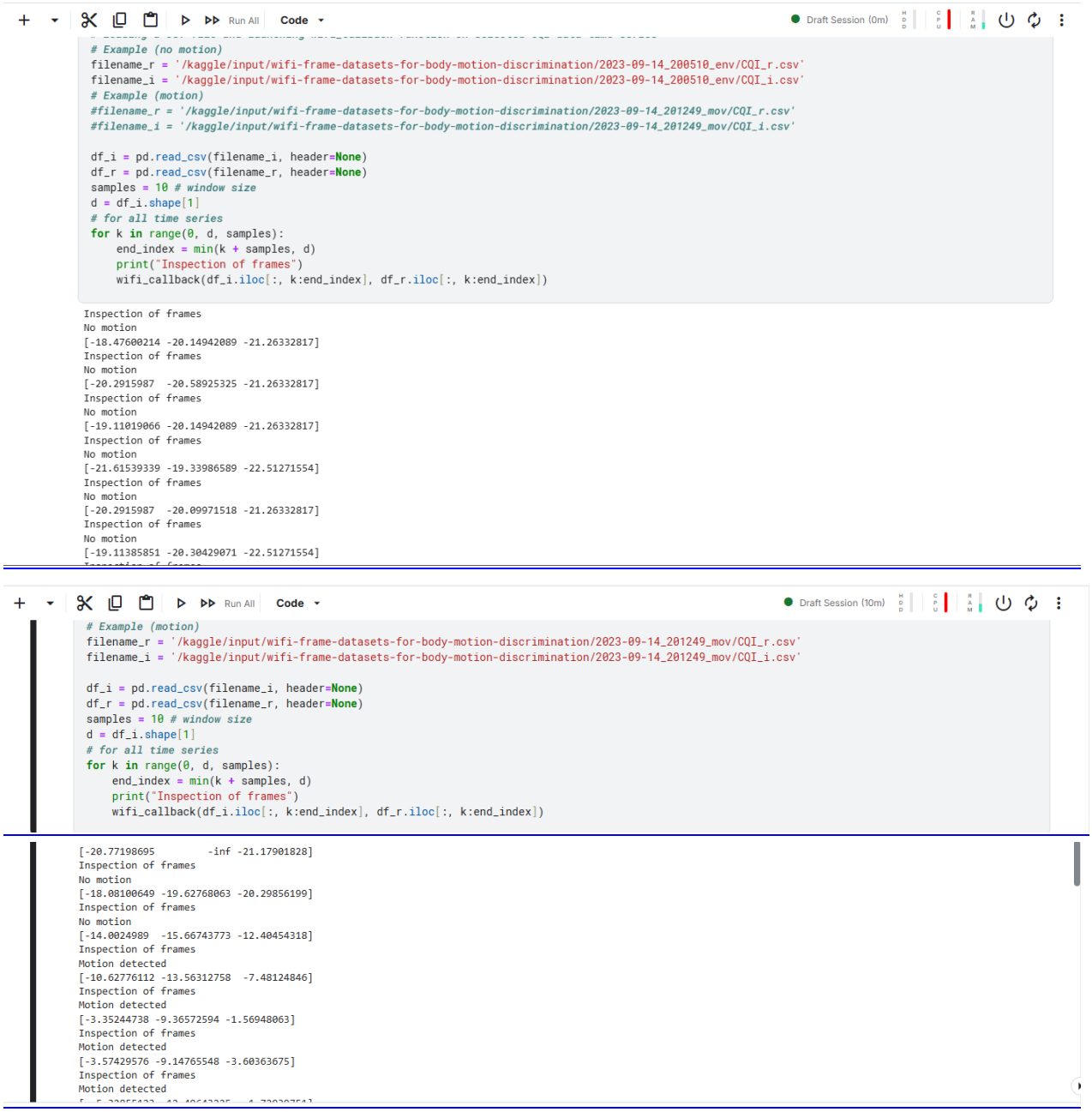

```
# Example (no motion)
filename_r = '/kaggle/input/wifi-frame-datasets-for-body-motion-discrimination/2023-09-14_200510_env/CQI_r.csv'
filename_i = '/kaggle/input/wifi-frame-datasets-for-body-motion-discrimination/2023-09-14_200510_env/CQI_i.csv'
# Example (motion)
#filename_r = '/kaggle/input/wifi-frame-datasets-for-body-motion-discrimination/2023-09-14_201249_mov/CQI_r.csv'
#filename_i = '/kaggle/input/wifi-frame-datasets-for-body-motion-discrimination/2023-09-14_201249_mov/CQI_i.csv'

df_i = pd.read_csv(filename_i, header=None)
df_r = pd.read_csv(filename_r, header=None)
samples = 10 # window size
d = df_i.shape[1]
# for all time series
for k in range(0, d, samples):
    end_index = min(k + samples, d)
    print("Inspection of frames")
    wifi_callback(df_i.iloc[:, k:end_index], df_r.iloc[:, k:end_index])
```

```
Inspection of frames
No motion
[-18.47600214 -20.14942089 -21.26332817]
Inspection of frames
No motion
[-20.2915987  -20.58925325 -21.26332817]
Inspection of frames
No motion
[-19.11019066 -20.14942089 -21.26332817]
Inspection of frames
No motion
[-21.61539339 -19.33986589 -22.51271554]
Inspection of frames
No motion
[-20.2915987  -20.09971518 -21.26332817]
Inspection of frames
No motion
[-19.11385851 -20.30429071 -22.51271554]
```

```
# Example (motion)
filename_r = '/kaggle/input/wifi-frame-datasets-for-body-motion-discrimination/2023-09-14_201249_mov/CQI_r.csv'
filename_i = '/kaggle/input/wifi-frame-datasets-for-body-motion-discrimination/2023-09-14_201249_mov/CQI_i.csv'

df_i = pd.read_csv(filename_i, header=None)
df_r = pd.read_csv(filename_r, header=None)
samples = 10 # window size
d = df_i.shape[1]
# for all time series
for k in range(0, d, samples):
    end_index = min(k + samples, d)
    print("Inspection of frames")
    wifi_callback(df_i.iloc[:, k:end_index], df_r.iloc[:, k:end_index])
```

```
[-20.77198695         -inf -21.17901828]
Inspection of frames
No motion
[-18.08100649 -19.62768063 -20.29856199]
Inspection of frames
No motion
[-14.0024989  -15.66743773 -12.40454318]
Inspection of frames
Motion detected
[-10.62776112 -13.56312758  -7.48124846]
Inspection of frames
Motion detected
[-3.35244738 -9.36572594 -1.56948063]
Inspection of frames
Motion detected
[-3.57429576 -9.14765548 -3.60363675]
Inspection of frames
Motion detected
```

Fig. 6. Examples of the source code for testing MUSIC processing system. No motion example (top), motion detection (bottom). The MUSIC system uses 3 antennas at the AP, 3 transmit antennas and one optimized beampattern.

Further details will be provided in WP6 and D6.4

4.2. WiFi devices and Channel Quality Information

All MIMO WiFi devices are configured in monitor mode and working in the 5.32 GHz band (i.e., WiFi band 2, channel 64, OFDM symbol sub-carrier spacing 312.5 kHz and nominal bandwidth equal to 20 MHz). The monitor mode allows the receivers to observe the CSI values on the considered channel without explicit IP handshaking procedures. The TX device is programmed to inject (i.e., transmit) custom IEEE 802.11n PHY Protocol Data Units (PPDU) structured as standard

High-Throughput (HT) greenfield WiFi format including preamble, MAC addresses, header and payload: injected frames are sent at regular time intervals of 10 ms. In our tests, the TX device acts as an access point while the RX devices are collecting and measuring CQI reports. For each transmitter-receiver pair we obtain the CQI reports of 30 pilot subcarriers. The adopted chipset is the Intel Wireless Link 5300 working as a MIMO-OFDM baseband modem. CQI reports are organized into several CSV files as described in the following. Each CSV file tracks the CQI data set, organized by frequency, antenna and time frames.

4.3. Folders and CSV files

Each folder corresponds to a different body activity. In particular: 1) CQI_dB.csv contains dB converted power measurements, 2) CQI_i.csv contains the corresponding imaginary components of the channel state information after phase unwrapping 3) CQI_r.csv contains the corresponding real components of the channel state information after phase unwrapping

4.4. File and columns CSI datasets descriptions

Each CSV file has dimension 270 x T, The T columns represent the (variable) number of consecutive WiFi frames (time series). The 270 rows represent the CQI samples obtained for each WiFi frame. Rows i identify the TX antenna, the RX antenna and the specific pilot SUBCARRIER and are organized as follows:

ROW	**TX NUMBER**	**RX NUMBER**	**SUBCARRIER**	**ANTENNA PATTERN**
i=1	TX 1	RX 1	SUBCARRIER 1	ID1
i=2	TX 2	RX 1	SUBCARRIER 1	ID1
i=3	TX 3	RX 1	SUBCARRIER 1	ID1
i=4	TX 1	RX 2	SUBCARRIER 1	ID1
i=5	TX 2	RX 2	SUBCARRIER 1	ID1
i=6	TX 3	RX 2	SUBCARRIER 1	ID1
i=7	TX 1	RX 3	SUBCARRIER 1	ID1
i=8	TX 2	RX 3	SUBCARRIER 1	ID1
i=9	TX 3	RX 3	SUBCARRIER 1	ID1

i=10	TX 1	RX 1	SUBCARRIER 2	…
i=11	TX 2	RX 1	SUBCARRIER 2	…
i=12	TX 3	RX 1	SUBCARRIER 2	…
…	…	…	…	…
i=270	TX 3	RX 3	SUBCARRIER 30	…
i=271	TX1	TX1	SUBCARRIER 1	ID2
…	…	…	…	…
i=540	TX3	RX3	SUBCARRIER 30	ID2

It should be noted that in the case where multiple patterns per antenna are used (a case that will be covered in WP6 and D6.4), each CSI observation on each antenna and subcarrier will be replicated for each beam steering profile (ID xx). Transmit and Received antenna might have arbitrary number depending on the AP and Client WiFi hardware.

The attached code provides an example for the evaluation of MUSIC spectrum (see figure below)

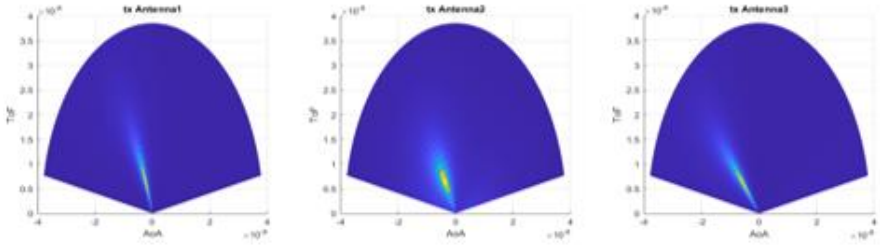

Fig. 7. Illustration of 3 MUSIC spectra obtained on a receiver equipped with 3 antennas. Each MUSIC spectrum refers to a different TX antenna and is visualized in terms of range (or time of flight – ToF) and azimuth (or Angle of Arrival – AoA).

5. References

[1] NanoRFE VNA6000-A. [Online]. Available: https://nanorfe.com/vna6000.html.

[2] S. Savazzi, V. Rampa, S. Kianoush and D. Piazza, "Pattern reconfigurable antennas for passive motion detection: WiFi test-bed and first studies," *2019 IEEE 30th Annual International Symposium on Personal, Indoor and Mobile Radio Communications (PIMRC)*, Istanbul, Turkey, 2019, pp. 1-6, doi: 10.1109/PIMRC.2019.8904262.

6. Table of Figures

Fig. 1. Wide-angle photograph of the planar scanner (dense 2D array of antennas) installed in an office at TUM..... 9

Fig. 2. Typical measured transmission data within the office environment. Illustration of the magnitude of the transmission (left) in dB and the corresponding phase information (right) in degree..... 10

Fig. 3. Female and male mannequins used for the measurements. 10

Fig. 4. Illustration of a holographic three-dimensional image generated from the difference of the datasets "mannequin_08_04_06_2024.mat" and "mannequin_07_03_06_2024.mat". On the top, a point-cloud illustration of the dominant scatterers is shown. Projections to the plane of the measurement surface (xy-plane, top-right-top), a vertical cut (xz-plane, top-right-bottom) and a cross-section projection (yz -plane, top-left-bottom) are provided. The arrangement of measurement "mannequin_08_04_06_2024" is shown in the photograph on the bottom. 12

Fig. 5. Illustration of the CSI data structuring of a MIMO WiFi link. 3D CSI structures are defined in terms of frequency (subcarriers), symbols and antennas (TX-RX pair)..... 14

Fig. 6. Examples of the source code for testing MUSIC processing system. No motion example (top), motion detection (bottom). The MUSIC system uses 3 antennas at the AP, 3 transmit antennas and one optimized beampattern. 16

Fig. 7. Illustration of 3 MUSIC spectra obtained on a receiver equipped with 3 antennas. Each MUSIC spectrum refers to a different TX antenna and is visualized in terms of range (or time of flight – ToF) and azimuth (or Angle of Arrival – AoA). 18